

Appendix: ***Modeling One-Dimensional X-Ray Patterns***

We describe a model for the calculation of one-dimensional X-ray diffraction patterns for the clay minerals. It applies to mixed-layered as well as to simple structures. There is not enough information in this section to allow you to sit down and write your own program for mixed-layered clay minerals, but if you study the key references (Reynolds, 1980; James, 1965; Bethke and Reynolds, 1986), you should be able to do just that. You should be able to construct a model like this for the simple clay minerals by using Eqs. (3.9), (3.13), (3.14), and (3.15) as a start and then adding refinements discussed in this Appendix. A program called NEWMOD[©] that does all the things discussed below is commercially available (Reynolds, 1985).

Calculated diffraction patterns are useful for both instruction and research. It takes a very long time for the beginning clay scientist to encounter and interpret diffraction patterns from a wide range of simple and mixed-layered clay minerals. But they can be computed and studied, and this is a very fast alternative. Experiments with compositional variations reinforce intuition or teach the effects of these variations on the patterns. For example, you can quickly answer the questions: What is the effect of increasing Fe substitution on the intensity ratio of the 002/005 reflections for illite? What happens to the basal diffraction pattern of a mica if large amounts of Li are assumed to be in octahedral coordination? For the mixed-layered clay minerals, such questions are almost endless, and answering at least a few of them by means of calculated patterns will greatly increase the effectiveness of the investigator.

At the research level, calculated patterns are invaluable for estimating the composition of simple clay minerals; for identifying, working out the composition, and identifying ordering types for mixed-layered clay minerals; and for generating standard intensities for quantitative standardization (Chapter 9). The limit is not yet in sight. As computers become faster and memory is increased, existing models will be refined further and will run fast enough to be usable in truly interactive modes. Modeling will lead the way toward the identification and quantification of more complicated structures such as mixed-layered clay minerals that contain more than two components.

THE INPUT VARIABLES***Simulating the Instrument***

A realistic model of a diffraction pattern requires that you specify all the important mineral structural data, and that you know the values and settings that describe the optical configuration of the diffractometer being simulated. There are a good many instrumental variables. They are listed in Table A.1.

Table A.1. Instrumental variables

Lambda	1.5418
Divergence slit	1.0
Goniometer radius	20
Soller slit 1	6.6
Soller slit 2	2.0
Sample length	3.6
Quartz reference intensity	25,000

Lambda (λ) is the wavelength of the incident radiation in Ångstrom units. $\text{CuK}\alpha$ is most commonly used in the United States, and $\text{CoK}\alpha$ is favored in Europe, but other wavelengths can be used. The divergence slit controls the beam divergence expressed in degrees for the primary, incident X-ray beam. This quantity is needed, in conjunction with values for the goniometer radius and the sample length, in order to correct for the intensity loss at low diffraction angles caused by an illumination spot whose length exceeds that of the sample. Values for the goniometer radius and the sample length are expressed in centimeters. Angular values in degrees are shown for the two Soller slits or, if only one is used, for the effective aperture or axial divergence of the radiation tunnel that has no slit. The latter is 6.6° for the Siemens D-500, and that value is probably acceptable for other instruments with one “missing” Soller slit. Soller slit 1 is the primary or incident beam slit, and Soller slit 2 is the diffracted beam slit. Calculation of the Lorentz factor requires values for the Soller slits and the preferred orientation of crystallites in the sample.

The quartz reference intensity denotes the peak intensity in counts per second for the reflection from a randomly oriented quartz powder at $d = 3.34$ Å. This measurement must be made on the goniometer with which the results from the program are to be compared, and the goniometer setup must be the same as that described by the parameters for the calculation. The quartz reference intensity is required for the calculation of absolute intensities.

Describing the Clay Mineral

A useful inventory of clay mineral types for a diffraction model such as NEWMOD[®] consists of illite, biotite, kaolinite, serpentine, tri-tri-chlorite, two-water-layer di-smectite, two-water-layer tri-smectite, two-glycol-layer-di-

smectite, two-glycol-layer tri-smectite, one-water-layer di-smectite, one-water-layer tri-smectite, two-water-layer Mg-vermiculite, and one-glycol-layer Na-vermiculite. You might also consider adding di-di-chlorite, di-tri-chlorite, and tri-di-chlorite. The compositions of all these, save kaolinite, are variable, and the model must have a provision for defining their compositions.

The items in Table A.2 describe the variables needed for modeling X-ray diffraction patterns of clay minerals. The default values are good averages, and the ranges are the most common. Use of these values will produce line breadths that realistically simulate those of many natural samples. We offer a few words about each value. The exchange capacity for smectites is required, and it is conveniently expressed as the number of univalent exchangeable cations per $(\text{Si,Al})_4$. Options should be available for specifying the exchange cation in smectites, and Na, K, Mg, Ca, and Sr are useful choices. Ca is a good default ion. The Fe content must be specified for the octahedral sheets in dioctahedral and trioctahedral minerals, and for chlorites; Fe must also be specified for the hydroxide interlayer. The number of atoms of K is needed for modeling illite, and, as described later, this value can be manipulated to simulate Na for paragonite and NH_4 for ammonium illite. Modeling of the diffraction patterns for pyrophyllite and talc requires the value of zero here. Smectites and vermiculites have interlayer complexes of exchangeable cations and water or ethylene glycol. These complexes have a definite atomic structure that must be built into the calculation by extension of the unit cell formulation for G (Eq. 3.9) beyond the hexagonal oxygen surface plane of the silicate layer.

The quantity μ^* is the mean sample mass absorption coefficient, and 45 is a realistic average value for low-Fe clay minerals irradiated by $\text{CuK}\alpha$. μ^* controls only absolute intensities, and σ^* is the standard deviation of a Gaussian orientation function for the crystals in the powder aggregate. It may be measured for the most accurate work, such as quantitative analysis or one-dimensional structure determinations for the clay minerals (Reynolds, 1986). The σ^* , in conjunction with the Soller slits, controls both absolute intensity and angle-dependent intensity through the Lorentz factor. High N and low N refer, respectively, to the number of unit cells stacked in the Z direction that make up the largest and smallest crystallites. A range of N is used here to eliminate the spurious ripples between peaks of the interference function (see Fig. 3.14).

The quantity $q(N)$ describes the crystallite size distribution. In other words, if, within the range of N specified, we want crystallites 9 unit cells thick to constitute 22% of the crystallites, then $q(9) = 0.22$. For routine calculations of diffractograms or quantitative standardization, set all values of $q(N)$ to the same value [see Eq. (3.15), p. 92]. Note, however, that $q(N)$ must be normalized to unity by dividing each initial value of $q(N)$ by the sum of the initial values for $q(N)$. If peak shape is to be modeled, then you can experiment with the defect-broadening option that requires a value for δ , the mean defect-

free distance.

Table A.2. Default chemical, structural, and sample variables

Exchange capacity	0.35
Exchange cation	Ca
Fe atoms per 2 or 3 octahedral sites	0-2, 0-3
K per 12-fold site	0-1
Interlayer complex	1-water, 2-glycol layers, etc.
μ^*	45
σ^*	12
Low N	3
High N	14
$q(N)$	1
δ	Variable
Proportion of component 1 ^a	0-1
Reichweite ^a	0, 1, 2, 3

^aApplies to mixed-layered clay minerals.

The distance δ is the average distance in a crystal that is not interrupted by a stacking fault that breaks the crystal into two or more X-ray coherent scattering domains. The defect-broadening option produces a special kind of particle-size distribution that, as you will see when you try it, generates very realistic looking peak shapes, particularly for pure minerals. More on this subject later.

Mixed-layered clay minerals require two parameters: a compositional parameter that fixes the relative amounts of each of the two mineral types in the interstratification, and a numerical statement that describes the ordering rules for the sacking sequence along Z (the Reichweite). Let the two types of layers be A and B . Only one of these need be specified by a decimal fraction between 0 and 1 because the sum of the decimal fractions of the two is equal to unity ($P_A + P_B = 1$). Reichweite values that seem to have natural significance at the present time are 0, 1, 2, and 3.

THEORY

Earlier published work by Reynolds (e.g., Reynolds, 1980; Reynolds and Hower, 1970) used a simplification in the mathematics that limited the algorithm to mixed-layered clay minerals that have unit cells centrosymmetric on projection to Z . To handle additional clay mineral types such as kaolinite and serpentine, we need a general formulation of the intensity equation such as that given by Eqs. (A.1) and (A.2):

$$I = Lp \sum_S G_j^* G_k \sigma_s (\cos \phi S + i \sin \phi S) \quad (\text{A.1})$$

$$\phi = (4\pi \sin\theta) / \lambda \quad (\text{A.2})$$

The G subscripts identify the layer types that are separated by the spacing S . The layer transforms G originate at the center of the lowermost oxygen plane of the tetrahedral sheet (Fig. A.1). Lp is the Lorentz-polarization factor described later. S is the value of a spacing, in Ångstroms, defined by the number of layers stacked along Z (see Fig. A.1). G_j^* is the complex conjugate of the layer transform of layer A or B , and G_k is the transform of layer type A or B .

By way of review, let some arbitrary variable

$$U = X\cos a + i Y\sin b; \text{ then } U^* = X\cos a - i Y\sin b$$

where $i = \sqrt{-1}$. If you do the multiplications of Eq. (A.1) correctly, all the imaginary components will cancel out, i.e., all occurrences of i will be gone. The summation of Eq. (A.1) is taken over all values of S including the limit $S = 0$ (single layers). σ_S is the frequency of occurrence of the spacing S . It is this quantity that greatly complicates the calculation of diffraction patterns for mixed-layered clay minerals. We cannot go into this sufficiently here to allow you to do the calculations, but a few comments should give you the main ideas. The interested reader is referred to Reynolds (1980) and Bethke and Reynolds (1986) for details.

The frequency term consists of two parts. The first part consists of the number of times that a given array fits into a crystallite that has N layers. The array shown by Fig. A.1 contains five layers, and it will fit only once into a five-layered crystallite. It will fit twice into a six-layered crystallite, three times in a seven-layered crystallite, etc. The rule, then, is to multiply the probability of occurrence by $N + 1$ minus the number of layers in the array. The probability is the complicated part. Figure A.1 shows only one array out of all the possible combinations and permutations. Suppose that $N = 10$. Then there are 2^{10} such arrays containing 10 layers, 2^9 containing 9, etc., and 2^5 (32) that contain 5 layers. We consider one of the 32 in Fig. A.1. The other arrays in this example are ignored that contain 2, 3, 4, 6, 7, 8, 9, and 10 layers. Let the proportion of type A in the assumed mixed-layered clay mineral be 0.7 (for example); then $P_A = 0.7$ and $P_B = 0.3$ because $P_A + P_B = 1$. If the interstratification is random (i.e., $R = 0$), then the probability of occurrence is simply P_A^3 times P_B^2 , where the numbers in the exponents refer, respectively, to the numbers of A and B layers in the array. σ_S for this term of the summation is $5 \times (0.3^2 \times 0.7^3) = 0.1544$. Suppose now that $R = 1$. Then we need to compound the conditional or transitional probabilities for this array. Proceeding upward from the bottom, we have

$$\sigma_S = 5(P_B P_{B.A} P_{A.A} P_{A.B} P_{B.A}) \quad (\text{A.3})$$

To make this calculation, however, we need values for the conditional

probabilities $P_{B,A}$, $P_{A,A}$, etc. Read these as “the probability of an A following a B ,” and “the probability of an A following an A .” We have touched on this subject in Chapter 5 (Box 5.3, p. 173), but more detail is needed here. If $R = 1$ and the composition of the mixed-layered mineral is greater than 50% A , then a B -type layer cannot follow a B -type layer. In other words, $P_{B,B} = 0$. Note that $P_{B,A} + P_{B,B} = 1$ because something must follow a B . It follows then that $P_{B,A} = 1$. So far, we have the transitional probabilities $P_{B,A}$ and $P_{B,B}$, and we need $P_{A,B}$ and $P_{A,A}$ to finish the calculation. The probability of occurrence of the pair AB is equal to the probability of an A times the probability of a B following an A , or $P_A P_{A,B}$. The probability of occurrence of the pair AB is equal to that of the pair BA , and the latter is equal to $P_B P_{B,A}$. So we write

$$P_A P_{A,B} = P_B P_{B,A}$$

or

$$P_{A,B} = P_B P_{B,A} / P_A = 0.3 \times 1 / 0.7 = 0.4286$$

and

$$P_{A,B} + P_{A,A} = 1$$

so

$$P_{A,A} = (1 - 0.4286) = 0.5714$$

We can now calculate σ_S from Eq. (A.3):

$$\sigma_S = 5 \times 0.3 \times 1 \times 0.5714 \times 0.4286 \times 1 = 0.3674$$

Notice that σ_S is larger for the $R1$ structure than for the $R0$ type. The reason is that we have described an array that has three interfaces of the types A,B and B,A , and these types are favored by the condition of nearest-neighbor

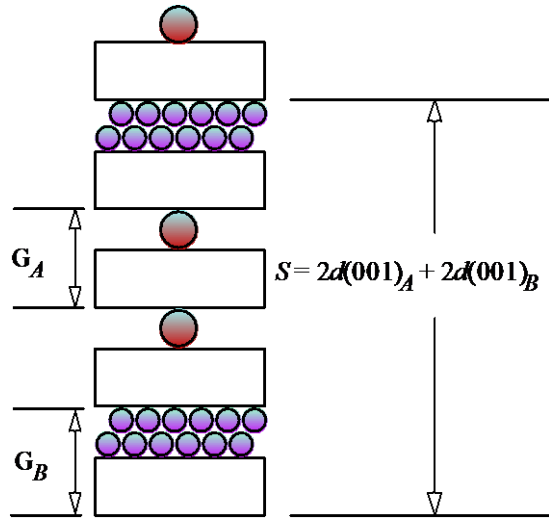


Fig. A.1. One of the possible spacings S formed by a core of two A type layers and one B type layer, with a B on one end and an A on the other.

ordering, which is the $R = 1$ structure. A different array (reading from bottom to top) $A-B-B-A-A$ also contains three A -type layers and two B types. For $R = 0$ it has the same frequency of occurrence as the example described before, but for $R = 1$, $\sigma_S = 0$. See if you can figure out why this statement is correct.

The calculation of σ_S is more involved for cases of $R > 1$ because you must compound long-range transitional probabilities such as $P_{AB.B}$ and $P_{ABA.A}$. If you wish to follow through on these cases, we refer you to the literature cited earlier.

The Lorentz-polarization factor is given by

$$L_p = \frac{(1 + \cos^2 2\theta) \Psi}{\sin \theta} \quad (\text{A.4})$$

where the cosine expression is the polarization factor, $\sin \theta$ is the single-crystal Lorentz factor, and ψ is the powder ring distribution factor. [We must avoid confusion here. In Eq. (3.12), the denominator was given as $\sin 2\theta$ for single crystals. This quantity is correct for the *integrated* intensity. $\sin \theta$ applies to the point-by-point intensity of a diffraction profile.] For a randomly oriented powder, ψ is proportional to $1/\sin \theta$; and for a single crystal, ψ is constant. Oriented clay aggregates present values of ψ that are intermediate to these special cases. The development of the theory is given by Reynolds (1986). The computation of ψ requires the root-mean-square angular divergence (in degrees) of the primary and diffracted beam Soller slits and a value for σ^* , which is the standard deviation of a Gaussian distribution that describes the frequency of occurrence of crystallites that are tilted by a given angle (ω) from the mean orientation, which is the orientation parallel to the surface of the powder aggregate. The powder ring distribution factor ψ controls angle-dependent intensity as well as absolute intensity. For this reason, well-oriented clay aggregates produce much stronger diffraction intensities than do poorly or randomly oriented aggregates. The absolute intensity at moderate and high angles is approximately proportional to $1/(\sigma^*)^2$. The derivations of the relevant equations and their applications are given by Reynolds (1986).

The calculated intensities are put on an absolute basis (I_0) by multiplying the calculated intensity values (I) by the quotient shown in Eq. (A.5) (Reynolds, 1983); \bar{d} is the weighted mean value of $d(001)$ for the two components; \bar{V} is the weighted mean volume of the unit cell; ρ is the mean density; μ^* is the sample mass absorption coefficient; and \bar{N} is the weighted mean of the crystallite size distribution, given by the two additional equations. *The constant K is a collection of physical constants, an empirical constant, and the quartz reference intensity. This collection accounts for instrument operating conditions.* The quartz reference intensity is the peak intensity, in counts per second, for the quartz (101) reflection at $d = 3.34 \text{ \AA}$. The measurement is made on a pure quartz powder or on one of the polycrystalline quartz aggregates commonly supplied by diffractometer manufacturers. The measurement must be made under the same operating conditions as those used

for the clay mineral diffraction patterns that are to be compared with the calculated results. Overall errors in the accuracy of I_0 amount to about 10% if μ^* and σ^* are measured (Reynolds, 1989).

$$I_0 = I \frac{Kd}{NV^2 \rho \omega^*} \quad (\text{A.5})$$

where

$$\bar{N} = \sum_N q(N)N$$

and

$$\sum_N q(N) = 1$$

The calculated intensities are corrected for the angle-dependent effects of a short sample and/or a long beam projection on the sample. These factors, coupled with the goniometer radius, cause progressively greater intensity losses at lower diffraction angles, and there is some angle above which such effects are absent. The length of the beam “footprint” on the sample, which is controlled by the primary divergence slit, is

$$LB = R_0 \alpha (\pi/180) / \sin\theta \quad (\text{A.6})$$

where R_0 is the goniometer radius in centimeters, α is the angular divergence of the primary divergence slit in degrees, and $\pi/180$ is the radian conversion. The calculated intensities are multiplied by the sample length in centimeters and divided by LB [Eq. (A.6)], only for angles at which LB exceeds the sample length.

Structures of the Component Layers

The layer transforms G are Fourier transforms of the atomic structure along the Z direction. Transform means change, of course, and these transforms effect a change from (1) the coordinates for the position of electrons in space to (2) the amplitude of scattering as a function of the angle of diffraction. Unit cell volumes are based on the half-unit cell, $(\text{Si,Al})_4\text{O}_{10}$, except for the 1:1 minerals, which are based on Si_2O_5 . Atomic scattering factors are calculated according to Wright (1973). Half-ionized atomic scattering factors are used for Si, Al, and silicate O, and fully ionized values are used for the other cations. Neutral atom (i.e., not ions) factors obtain for ethylene glycol. For water and OH^- the scattering factor is the sum of the factors for H^+ and O^{2-} . Debye-Waller temperature corrections for atomic vibrations are computed using $B = 1.5$ for cations and $B = 2$ for anions. $B = 11$ is used for ethylene glycol

molecules and for one of the water molecule sites in the two-layered water-smectite structure. B is a measure of the mean square displacement of an atom from its ideal place in the structure. It is used to adjust the atomic scattering factor in this form (the higher the temperature, the greater the displacement, the less efficient the scattering)

$$f = f_0 \exp(-B \sin^2\theta / \lambda^2) \quad (\text{A.7})$$

Equation (A.7) shows how B is applied. The quantity f_0 is the scattering factor for an atom or ion at rest, and f is the temperature-corrected value.

NEWMOD[©] uses three 2:1 silicate layer structures. The dioctahedral layer is based on unpublished work by Bridges and Reynolds on illite and is used for all the dioctahedral components except smectite, which is taken from Reynolds (1965). All trioctahedral 2:1 layers are defined by a structure published by Mathieson and Walker (1954) for vermiculite. Kaolinite atomic coordinates are those of Zvyagin (1960), and serpentine has the generalized 1:1 trioctahedral structure described by Bailey (1969). The two-layered ethylene glycol structure is taken from Reynolds (1965) and the one-layer Na ethylene glycol structure from Bradley et al. (1963). The two-layered water structure (smectite) is based on unpublished work by Hower and Reynolds, and the one-layered water structure (smectite) assumes that exchangeable cations and water molecules are located at the center of the interlayer space. The water content of the latter is based on the data of Mooney et al. (1952). Atomic coordinates for the trioctahedral chlorite hydroxide sheet are given by Brindley (1961a), and the dioctahedral chlorite hydroxide interlayer has the Al-OH separation of a generalized kaolinite structure (Brindley, 1961b). The two-layered water vermiculite interlayer structure is taken from Mathieson and Walker (1954).

Some of the interlayer structures are only educated guesses. However, small errors in atomic positions cause only small discrepancies in intensities at intermediate and low diffraction angles where most clay mineral work is done. But if you use these data to calculate intensities at angles as high as $50^\circ 2\theta$ and beyond ($\text{CuK}\alpha$), be advised that the intensity results are accurate only if the calculations involve the better-known components such as illite, biotite, two-layered glycol smectite, two-layered water vermiculite, tri-tri-chlorite, and kaolinite.

Table A.3 shows the atomic coordinates for the silicate 2:1 skeletons with respect to an origin at the center of the octahedral sheet (Fig. 3.20, p. 98). Atomic coordinates for interlayer complexes have as their origin ($Z = 0.00$) the center of symmetry on projection to Z for the interlayer structure. Only half of each structure is given, and for the sites not on the center of symmetry, the numbers of atoms in each are doubled. This location of the origin gives a

Table A.3. One-dimensional atomic structures of silicate layers; coordinates are in Ångstroms measured perpendicular to $d(001)$ along Z

2:1 Di-silicate ^a		Di-smectite		2:1 Tri-silicate	
3.300	6 O	3.27	6 O	3.27	6 O
2.720	4 Si	2.70	4 Si	2.75	4 Si
1.065	4 O + 2 OH	1.06	4 O + 2 OH	1.06	4 O + 2 OH
0.000	1.7 (Fe, Al) + 0.3 Mg	0.00	0.7 (Fe, Al) + 0.3 Mg	0.00	3 (Fe,Mg)

1:1 Tri-silicate		Kaolinite	
4.32	3 OH	4.369	1 OH
3.31	3 (Fe,Mg)	4.311	2 OH
2.27	2 O + OH	3.396	1 Al
0.58	2 Si	3.382	1 Al
0.00	4 O	2.288	1 O + 1 OH
		2.274	1 O
		0.651	1 Si
		0.636	1 Si
		0.150	1 O
		0.143	1 O
		0.000	1 O

^aExcept for dioctahedral smectite.

coordinate reference that is most useful for calculating diffraction patterns using the approach demonstrated in Chapter 3 (Fig. 3.20 and associated discussion). To calculate G for any of the centrosymmetric minerals, calculate G for the silicate skeleton (G_S) and G for the interlayer material (G_I). G for the skeleton plus the interlayer is given by $G = G_S + G_I \cos(4\pi [d(001) / 2] \sin\theta / \lambda)$. The coordinates are given in the present form for simplicity, but you will have to transform them if you deal with mixed-layered clay minerals and use the noncentrosymmetric origin shown in Fig. A.1. The kaolinite and serpentine zero coordinates lie at the center of the basal oxygen sheet or oxygen atom of the 1:1 layer. Table A.4 lists the atomic coordinates and atomic compositions of the interlayer structures dealt with by NEWMOD[©].

ADVANCED TECHNIQUES

The model represented by NEWMOD[©] has applications that might not be obvious from an examination of the input parameters. Some of these are described here.

Pure Minerals

Diffraction patterns of pure minerals are produced by interlayering a component with itself. The proportions and Reichweite (R) are irrelevant, but roundoff errors may be minimized if you select 50/50 proportions and $R = 0$.

Table A.4 One-dimensional atomic structure of interlayer material, mineral

names, and $d(001)$; coordinates are in Ångstroms measured perpendicular to $d(001)$ along Z

Illite $d(001) = 10.0$		Biotite $d(001) = 10.0$		Tri-tri-chlorite $d(001) = 14.2$	
0.00	0-1 K	0.00	0-1 K	1.02	6 OH
				0.00	3 (Fe, Mg)
2 EG; $d(001) = 16.9^a$		1 EG; $d(001) = 12.9^a$		2-Water; $d(001) = 15.0^a$	
2.33	1.7 CH ₂ OH ^c	0.95	0.35 Na	1.20	1.4 H ₂ O
1.38	1.7 CH ₂ OH ^c	0.45	2 CH ₂ OH ^c	1.06	0.69 H ₂ O
0.51	1.2 H ₂ O ^b			0.35	0.69 H ₂ O
				0.00	nM^+
1-Water; $d(001) = 12.4^a$			Mg-Vermiculite; $d(001) = 14.32$		
0.00	2 H ₂ O+ nM^+		1.06	4.32 H ₂ O	
			0.00	0.32 Mg	

^aInterlayer material for smectite. ^bSubstitute exchangeable cations for water here.

^cTemperature factor, $B = 11$.

Compositional Superstructures

The algorithm described here and used by NEWMOD[®] allows the specification of different chemical compositions for each of the layer types. Consequently, you can proceed in the fashion described here for a pure mineral and specify, for example, low Fe in one “component” and high Fe in the other. The calculated pattern will contain the weak compositional superstructure reflections between each of the normal reflections if $R = 1$. If $R = 0$, the result is identical to that of a pure mineral with the average Fe content in each component. Higher Reichweite designations may produce bizarre results whose natural significance should not be dismissed until we begin to look for structures like these.

Layer Types Not Specifically Included

Some imagination is required for the simulation of layer types that are not included in the menu. The examples given here illustrate the principles, but they do not exhaust the possibilities. Suppose you wish to calculate the pattern for interstratified talc/saponite. To simulate the talc, select biotite and enter zero for the K and Fe contents. Then change $d(001)$ for biotite from 10 to 9.33 Å. Pyrophyllite can be treated similarly, except that illite is selected and $d(001)$ is changed to 9.2 Å. You might worry that talc and pyrophyllite do not have tetrahedral Al substitution, whereas biotite and illite do. But such substitution has only a small effect on intensity because the scattering factors are very similar for Al^{1.5+} and Si²⁺.

Atom Types Not Incorporated in the Model

The atomic scattering factor at low and intermediate diffraction angles is proportional to the number of electrons in the atom or ion. To simulate, for example, ammonium illite, divide 10 by 18 to get 0.56, because NH_4^+ has 10 electrons and K^+ has 18. Select illite, enter 0.56 for K, and increase $d(001)$ to 10.32 Å. Paragonite is handled in identical fashion because, by chance, Na^+ also contains 10 electrons, except that in this case $d(001)$ is decreased to 9.66 Å. This method is useful for dealing with some exotic micas and for extending the range of exchangeable cations in smectites so that it includes Cs, Rb, Pb, Zn, etc. For exchangeable cations, the charge on the modified cation must be identical to that of the cation selected from the standard menu, or else you will need to alter the exchange capacity.

Defect Broadening

Defect broadening refers to diffraction line broadening caused by randomly distributed stacking faults along the Z direction. The theory is described by Ergun (1970), who applied it to carbons. The statistical occurrence of such defects is given by δ , which is the mean defect-free distance, given here by the number of unit cells that are contiguous without interruption. $\delta = 10$ means that, on the average, coherent scattering domains are 10 unit cells thick, smaller domains are more abundant, and larger ones less so. The probability of an optically coherent length δ is given by

$$q(N) = \exp[- (N-1) / \delta] \quad (\text{A.8})$$

The largest crystallites (high N) are assumed to be very large compared with δ , but the exponential term becomes so small at large N that for practical purposes the calculations need not extend beyond high $N = 7\delta$. Realistic values for clay minerals are from 6 to 10, so computations can require values of high N as large as 50. Such a calculation for mixed-layered clay minerals is feasible only because of the efficiency of the very fast statistical algorithm developed by C. Bethke (Bethke and Reynolds, 1986). Experience with this model for line broadening has shown that very realistic results are obtained for clay minerals by setting high $N = 5\delta$.

Defect broadening produces a special kind of particle-size distribution [Eq. (A.8)] that produces diffraction lines that have a Cauchy or Lorentzian shape, in contrast to the more Gaussian line shapes produced by the condition $q(N) = 1$. If you try the defect-broadening option, we believe that you will agree that the realistic line shapes produced (particularly for non-mixed-layered clay minerals) suggest that real clay minerals consist of fairly large crystallites that have a mosaic substructure. As high N is diminished from 7δ , the line shape becomes more and more Gaussian due to the presence of finite-crystallite-sized effects.

REFERENCES

- Bailey, S. W. (1969) Polytypism of trioctahedral 1:1 layer silicates: *Clays and Clay Minerals* **17**, 355-71.
- Bethke, C. M. and Reynolds, R. C., Jr. (1986) Recursive method for determining frequency factors in interstratified clay diffraction calculations: *Clays and Clay Minerals* **34**, 224-26.
- Bradley, W. F., Weiss, E. J., and Rowland, R. A. (1963) A glycol-sodium vermiculite complex: *Clays and Clay Minerals*, Proc. 10th Nat. Conf., Austin, Texas, Pergamon Press Inc., 117-22.
- Brindley, G. W. (1961a) Chlorite minerals: in Brown, G., ed., *The X-Ray Identification and Crystal Structures of Clay Minerals*: Mineralogical Society, London, 242-96.
- Brindley, G. W. (1961b) Kaolin, serpentine and kindred minerals: in Brown, G., ed., *The X-Ray Identification and Crystal Structures of Clay Minerals*, Mineralogical Society, London, 51-131.
- Ergun, S. (1970) X-ray scattering by very defective lattices: *Phys. Rev. B* **131**, 3371-80.
- James, R. W. (1965) *The Optical Principles of the Diffraction of X-Rays*: Vol. II of the Crystalline State: Series edited by Sir Lawrence Bragg, Cornell University Press, 664 pp.
- Mathieson, A. McL., and Walker, G. F. (1954) Crystal structure of Mg-vermiculite: *Amer. Minerol.* **39**, 231-55.
- Mooney, R. W., Keenan, A. C., and Wood, L. A. (1952) Adsorption of water vapor by montmorillonite: *Jour. Amer. Chem. Soc.* **74**, 1367-74.
- Reynolds, R. C., Jr. (1965) An X-ray study of an ethylene glycol-montmorillonite complex: *Amer. Minerol.* **50**, 990-1001.
- Reynolds, R. C., Jr. (1980) Interstratified clay minerals: in Brindley, G.W., and Brown, G., editors, *Crystal Structures of Clay Minerals and Their X-Ray Identification*, Monograph No. **5**, Mineralogical Society, London, 249-303.
- Reynolds, R. C., Jr. (1983) Calculation of absolute diffraction intensities for mixed-layered clays: *Clays and Clay Minerals* **31**, 233-34.
- Reynolds, R. C., Jr. (1985) *NEWMOD*® a Computer Program for the Calculation of One-Dimensional Diffraction Patterns of Mixed-Layered Clays: R. C. Reynolds, Jr., 8 Brook Rd., Hanover, NH.
- Reynolds, R. C., Jr. (1986) The Lorentz factor and preferred orientation in oriented clay aggregates: *Clays and Clay Minerals* **34**, 359-67.
- Reynolds, R. C., Jr. (1989) Principles and techniques of quantitative analysis of clay minerals by X-ray powder diffraction: in Pevear, D. R., and Mumpton, F. A., editors, *Quantitative Mineral Analysis of Clays*, CMS Workshop Lectures, Vol. **1**, The Clay Minerals Society, 4-36.
- Reynolds, R. C., Jr., and Hower, J. (1970) The nature of interlayering in mixed-layered illite-montmorillonites: *Clays and Clay Minerals* **18**, 25-36.
- Wright, A. C. (1973) A compact representation for atomic scattering factors: *Clays and Clay Minerals* **21**, 489-90.
- Zvyagin, B. B. (1960) Electron diffraction determination of the structure of kaolinite: Soviet Physics, *Crystallography* **5**, 32-42.